INTERNATIONAL DESIGN CONFERENCE – DESIGN 2020
https://doi.org/10.1017/dsd.2020.44

OPTIMISATION OF WELDED BEAMS: HOW COST FUNCTIONS AFFECT THE RESULTS

D. Miler ✉, M. Hoić and D. Žeželj

University of Zagreb, Croatia

✉ daniel.miler@fsb.hr

Abstract

The increasing market competitiveness and CAE availability require the products to be optimised. This practice is exceedingly present when producing semi-standard parts like structural elements. Several cost calculation methods are developed, bringing up the question - which one to use? In this article, we compared three methods; a welded I-section beam was used as an example. The optimisation was carried out using two objectives (mass and cost) and was submitted to Eurocode boundary conditions. The results have shown that the cost calculation method has a negligible influence on the results.

Keywords: design optimisation, design practice, cost management

1. Introduction

The utility of optimisation in engineering design is indisputable. Implementing the optimisation phase in the product development process helps designers to reduce costs and enhance product performance. By introducing knowledge through the form of mathematical models, results are found quickly. Besides, with the development of easy-to-use algorithms, usage of optimisation is on the steady increase. The problem which remains is the quality of results - they are only as good as the mathematical model. Creating a comprehensive mathematical model is generally the most time-consuming task. It includes problem description and collection of associated data, variable selection, and formulation of objectives and boundaries (Arora, 2017).

While the boundaries are often based on governing technical standards, objective functions and their complexity are depending on the optimisation aim; whether it is to reduce the weight, volume, or power losses. Using weight or volume is straightforward, but in more complex objectives there are often several expressions available. Examples include cost calculation (Mela and Heinisuo, 2014), frictional power losses (Miler et al., 2018), and engine fuel consumption (Sawulski and Ławryńczuk, 2019). Thus, the choice of objective function could cause variations in the solutions.

In the crane design, various objective functions are employed to find the optimal solutions. The weight and beam cross-section surface are the most frequently used objective functions, with most of the studies carried out using a single objective. Ozbasaran (2018) presented the procedure for the optimal design of prismatic I-section beams, along with the necessary constraints. The section volume was used as the objective function. The examples also include the overhead gantry crane optimisation by Ahmid et al. (2017), where the authors used cross-section surface area as objective. The results were validated using the finite element method (FEM).

In addition to the cross-section surface, volume, or weight, the manufacturing cost is also frequently used as the objective function. Jarmai and Farkas (1999) presented a method for cost calculation of welded steel structures; the optimisation of a welded box beam was used as an example. A similar study was carried out by Pavlovčič et al. (2004), although with a more comprehensive cost calculation method. Mela and Heinisuo (2014) carried out a study to determine the performance of high strength steels as beam materials. The optimisation was carried out using the cost calculation based on the work by Haapio (2012) as an objective function.

In this article, studied how does the choice of mathematical models used to describe the same criterion affects the optimisation results. The welded steel beams were used as an example due to their wide-spread use and model availability. The optimisation process was structured as multi-objective; two objective functions were used - weight and cost. The expressions used for cost calculation were varied, aiming to solve the following research question:

> *How do different cost calculation methods affect the optimisation of mechanical structures?*

The manufacturing process of welded beams is described in Section 2 as it is necessary for the understanding of cost functions. The optimisation method, including the design variable selection, objective functions, and boundaries, is shown in Section 3. The algorithm selection, type, and properties are shown in the same section. The results are presented and discussed Section 4, along with the limitations and the outlook for future studies.

2. Problem overview

Beams of various cross-sections, sizes, and materials are used when designing steel structures. The beams are either rolled or produced by welding plates. Former are produced in standardised sizes of various cross-sections, resulting in a lower cost. The latter, despite the increased cost, offer more flexibility. The profiles are tailored according to the product requirements, allowing for geometric requirements or a decrease in weight.

In the case of gantry cranes, the increase in manufacturing costs due to using welded profiles is justified. It allows the engineer to optimise the design; for example, to reduce the weight or the surface area exposed to wind. With the decrease of mass, the inertial forces and self-weight caused stresses to fall as the beam weight reduces. Lower inertial forces allow for the selection of smaller driving mechanisms, which include gears

The welded beam production consists of several phases (Figure 1). Following the purchase of steel plates, each plate must be cut according to the required flange and web dimensions. Various cutting technologies are available, such as the flame (propane and oxygen were used in this study) or plasma cutting. Plate surfaces are then flattened and prepared for welding and painting; the surface of consistent quality is necessary to ensure welding effectiveness.

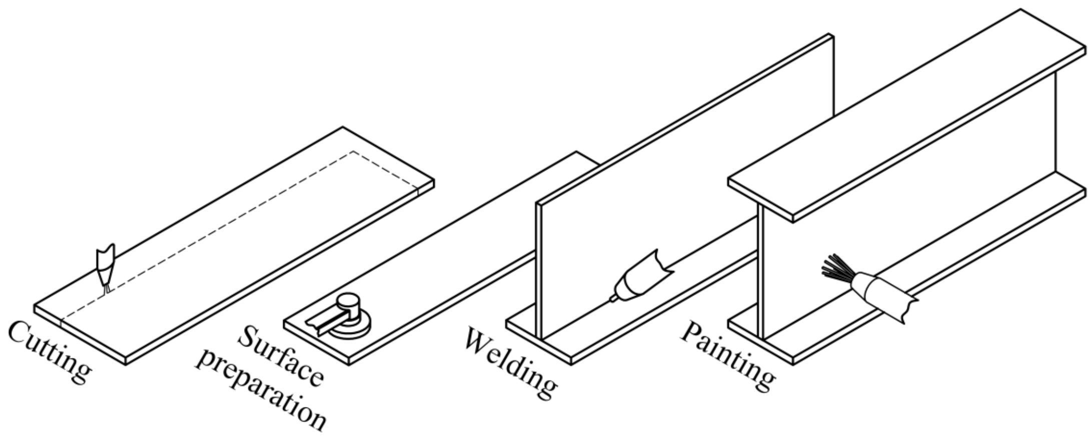

Figure 1. Welded I-profile manufacturing process

https://doi.org/10.1017/dsd.2020.44 Published online by Cambridge University Press

Plates are welded together next; in this article, we assumed that shielded manual arc welding (SMAW) process was used. Lastly, the beam is painted to provide corrosion resistance. Finally, it must be noted that supporting operations, such as the handling costs, additional fabrication costs (i.e. electrode changing), and non-productive times are not included in this overview, but are accounted for during the cost calculation (as required by each of the models).

3. Method

The optimisation procedure was structured by using a five-step formulation (Arora, 2017). First two steps, problem description and data collection, are covered in Section 2. This section includes step 3 (variable selection), step 4 (objective function formulation), and step 5 (boundary conditions). Additionally, the algorithm and associated properties that were used to carry out the optimisation process are shown. The resulting process is shown in the Figure 2.

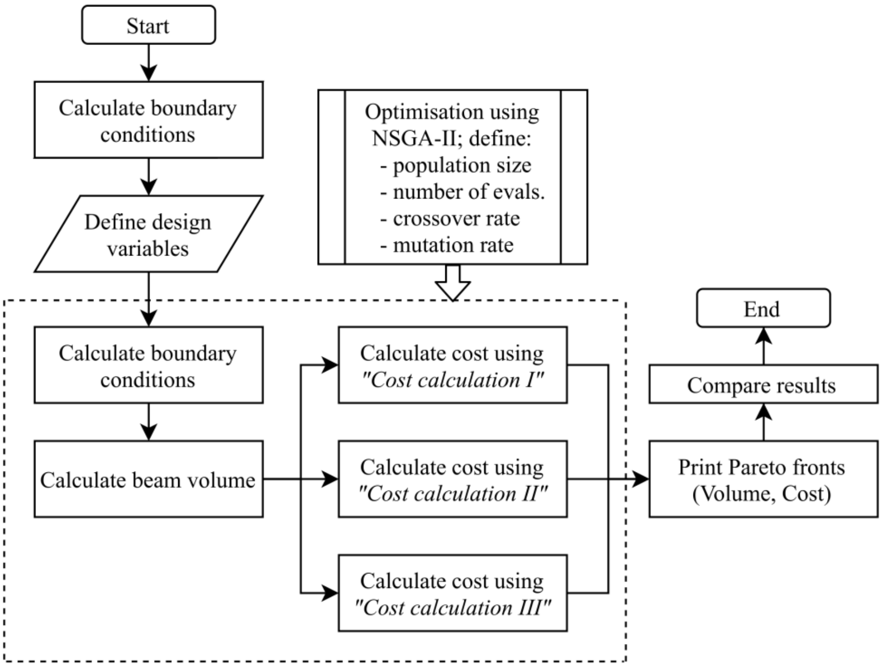

Figure 2. Optimisation process flowchart

The I-beam of a double-symmetric cross-section is considered (see Figure 3). The beam geometry is fully defined by four variables: flange width (b), flange thickness (t_b), web height (h), and web thickness (t_h). The resulting design variable vector is:

$$\mathbf{x} = \{b,\ t_b,\ h,\ t_h\}. \tag{1}$$

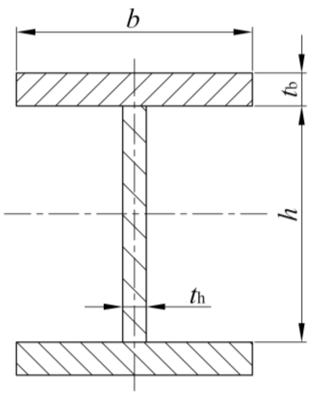

Design variable		*Minimum*	*Maximum*
Flange width	b, mm	100	1000
Flange thickness	t_b, mm	5	25
Web height	h, mm	5	25
Web thickness	t_h, mm	100	1000

Figure 3. Cross-section (left); design variables and their ranges (right)

https://doi.org/10.1017/dsd.2020.44 Published online by Cambridge University Press

The ranges of design variables were limited to reduce the share of unfeasible solutions from the initial consideration. The ranges are shown in Figure 3. Each flange is attached to the web through two fillet welds. The continuous welds were used to avoid stops and starts; thickness a_w = 4 mm was also kept constant.
The optimisation process was carried out using three sets of input data, which consisted of beam length L and load capacity Q:

- ***Set 1*** - beam length of 12 m and load capacity of 10,000 N;
- ***Set 2*** - beam length of 12 m and load capacity of 20,000 N;
- ***Set 3*** - beam length of 18 m and load capacity of 10,000 N.

3.1. Objective functions

Two objective functions were used - weight and cost. When designing cranes with greater reach, the ratio between self-weight and load capacity must be reduced. Thus, the beam weight is used as an objective function; its calculation process is trivial and is shown in Equation 2:

$$f_1(\mathbf{x}) = \left(2 \cdot b \cdot t_b + h \cdot t_h + 2 \cdot a_w^2\right) \cdot L; \quad (2)$$

The second objective function, manufacturing cost, was calculated using several different formulations (see Equations 3-5). For each of the formulations, the optimisation process was repeated, aiming to provide the basis for comparison.
The material cost is included in all three costing formulations and is calculated by multiplying beam weight with the material cost per unit. Since mass is already used as an objective function, it was not removed from the cost calculations as it tended to limit the ensuing Pareto front significantly. It also must be added that the focus is on the manufacturing cost, meaning that transportation and erection costs were not considered. Lastly, it should be added that variable definitions can be found in the Nomenclature section.

3.1.1. Cost calculation I (Jarmai and Farkas, 1999)

First of the assessed cost functions is one proposed by Jarmai and Farkas (1999). The authors have used time, which can later be multiplied with the corresponding cost factors, as function output. Same was done in this article; the objective function is written as:

$$f_{2\text{-}1}(\mathbf{x}) = \rho V + \frac{k_f}{k_m}\left(T_1 + T_2 + T_3 + T_4 + T_5 + T_6 + T_7\right); \quad (3)$$

The cost function $f_{2\text{-}1}(\mathbf{x})$ accounts for the influences of both the material and fabrication costs, including:

- welding times (T_1 - time for preparation, T_2 - time of welding, T_3 - additional time of fabrication; i.e. changing the electrode),
- plate flattening time T_4,
- surface preparation time T_5
- painting time T_6,
- the cutting and edge grinding time T_7.

3.1.2. Cost calculation II (Mela and Heinisuo, 2014)

The manufacturing cost calculation used by Mela and Heinisuo (2014) was based on the work presented by Haapio (2012). The authors have divided the manufacturing process into smaller segments, including the costs of labour, material, energy, and similar, with costs based on the ones typical for Finland. Variations caused by using different technologies were also included. Finally, the expression for cost calculation was given:

$$f_{2\text{-}2}(\mathbf{x}) = C_M(\mathbf{x}) + C_B(\mathbf{x}) + C_C(\mathbf{x}) + C_S(\mathbf{x}) + C_W(\mathbf{x}) + C_P(\mathbf{x}) \underbrace{+ C_T(\mathbf{x}) + C_E(\mathbf{x})}_{\text{not considered in this study}}; \quad (4)$$

https://doi.org/10.1017/dsd.2020.44 Published online by Cambridge University Press

In addition to the material costs, $f_{2\text{-}2}(\mathbf{x})$ accounts for the influences of blasting cost C_B, cutting cost C_C, sawing cost C_S, welding cost C_W, painting cost C_P, transportation cost C_T, and erecting cost C_E.

3.1.3. Cost calculation III (Pavlovčič et al., 2004)

The cost calculation function developed by Pavlovčič et al., 2004), similarly to the previous two considers both the material and manufacturing costs. Two numerical examples were provided, both of which have proven that besides the material, painting is the costliest manufacturing operation. The formulation is written as follows:

$$f_{2\text{-}3}(\mathbf{x}) = C_M + \sum C_W + \sum C_C + \sum C_P + \sum C_{SP} + \underbrace{\sum C_A + \sum C_J + \sum C_T + \sum C_T}_{\text{not considered in this study}}; \tag{5}$$

where C_{SP} is the cost of surface preparation, C_A cost of flange aligning, and C_J cost of joints. The remaining variables are indexed in accord with method II for the sake of simplicity.

3.2. Boundary conditions

The boundary conditions ensure that a solution is safe to use and technically viable. The safety and durability requirements regarding the steel structures are rigirous. Thus, for steel structures, it is necessary to ensure that strength and stability criteria are satisfied. Both are defined within the European standard (EN 1993-1, 2005) and for the task at hand include:

- resistance of cross-sections - bending moment, shear, bending and shear,
- buckling resistance (lateral-torsional buckling; uniform members in bending).

Additional crane design requirements are based on empirical knowledge and include:

- limited gantry beam deflection,
- balanced flange and web thicknesses.

All the boundary conditions included within the mathematical model are shown in Table 1.

Table 1. Applied boundary conditions

Condition	*Mathematical formulation*
Bending moment resistance	$M_{eD} - M_{c,RD} < 0; \quad M_{eD} = \frac{FQ \cdot L}{4} + \frac{G \cdot L}{8}, \quad M_{c,RD} = \frac{W_y(class) \cdot f_y}{\gamma_{M0}}.$
Shear resistance	$V_{eD} - V_{c,RD} < 0; \quad V_{eD} = \frac{W_y(class) \cdot f_y}{\gamma_{M1}}, \quad V_{c,rD} == \frac{0.5774 \cdot A_v \cdot f_y}{\gamma_{M0}}.$
Bending and shear resistance	Reduced plastic resistance moment calculated as: $M_{y,c,RD} = \frac{W_y(class) - \frac{\rho A_w^2}{4 \cdot t_h}}{\gamma_{M0}}.$ *Note: neglected if shear force is less than half the plastic shear resistance* (EN 1993-1, 2005).
Lateral-torsional buckling resistance	$M_{eD} - M_{b,RD} < 0; \quad M_{b,RD} = \chi_{LT} \frac{W_y(class) \cdot f_y}{\gamma_{M1}}.$
Deflection	$w - w_{perm} < 0; \quad w = \frac{F_Q \cdot L^3}{48 \cdot E \cdot I_y} + \frac{5 \cdot G \cdot L^3}{384 \cdot E \cdot I_y}, \quad w_{perm} = \frac{L}{600}.$
Flange and web thickness	$\left.\begin{array}{l} 1.2 \cdot t_h - t_b < 0 \\ t_b - 2 \cdot t_h < 0 \end{array}\right\} \; 1.2 \cdot t_h < t_b < 2 \cdot t_h.$

https://doi.org/10.1017/dsd.2020.44 Published online by Cambridge University Press

3.3. Algorithm

The objective functions are not smooth, making the use of gradient methods more difficult. Same was supported by an optimisation study carried out by Leng et al. (2011). Three optimisation methods were used to optimise the shape of an open cold-formed steel cross-section, aiming to increase the compressive strength. The authors compared the performance of the steepest descent method (gradient) and two stochastic algorithms (genetic algorithm and simulated annealing). Based on the results, the authors have concluded that the steepest descent method was dependant on the initial solution but offered good solutions. In the other hand, the stochastic methods covered the solution space more thoroughly at the price of increased computational cost.

Thus, in this article, the optimisation problem was solved using the stochastic method. NSGA-II (*non-dominated sorting genetic algorithm II*) was used due to its wide applicability and reliability (Deb et al., 2002). The population size n_{pop} = 500 was selected, along with the maximum number of generations (stopping criterion) n_{gen} = 300. The distribution index for the crossover of 20 was selected, while the distribution index for mutation was 100. In addition to genetic algorithm having ensured convergence, the process was replicated twice (number of runs n_{runs} = 3) to confirm that global optimum was found instead of the local one.

4. Results and discussion

The optimisation procedure was carried out three times for each of the sets. Different objective function for cost evaluation was used during each run. The calculation time was 63 s for each of the set-cost function combinations, which was acceptable. Thus, no additional algorithm/process optimisations aiming to reduce the computational cost were needed due to low running times.

The optimisation results are shown in Figure 4. The figure segments marked with a) and b) correspond to the set 1 solutions, parts c) and d) to the set 2 solutions, and parts e) and f) to the set 3 solutions. Furthermore, the web and flange plate dimensions are shown on the left side of the figure, while the corresponding plate thicknesses are shown on the right.

The set 1 solutions (Figure 4.a and 4.b) with the lowest weight correspond to the combination of largest plate widths and lowest flange thickness. As the mass increased, the flange width and web height gradually decreased, while the flange thickness increased. Moreover, Pareto optimal fronts corresponding to the set 1 are nearly identical for all the three cost calculation methods. The web thickness mostly remained the same.

The set 2 solutions (Figure 4.c and 4.d) follow the same trends regarding flange and web thicknesses; all three methods offer the same results. However, the web and flange plate widths were not uniformly selected by all three methods. In lower mass specimens (605 kg to 625 kg), cost calculation methods I (Jarmai and Farkas, 1999) and III (Pavlovčič et al., 2004) tended to select greater web height at the cost of flange width when compared to cost calculation method II (Mela and Heinisuo, 2014). Above 625 kg this behaviour persisted for method III, while the methods I and II were in consensus. Above 665 kg, all three methods offered similar results.

Regarding the set 3 solutions (Figure 4.e and 4.f), no influence of cost calculation method on the results was found. The selected web and flange thicknesses were the same, regardless of the method. Slight deviations were found in the region near the 1315 kg, but due to their limited magnitude, their impact is not significant.

Upon further inspection, the abrupt changes are found to be caused by a change in cross-section class. According to the European standard for the design of steel structures (EN 1993-1, 2005), profile cross-sections are divided into four classes. The design resistance of class 1 and 2 profiles is calculated using plastic section modulus, while its elastic counterpart is used in class 3. Specimens with higher web height to flange width ratio belong to the higher class. Thus, changes in the interval [605, 626] kg are caused by solution cross-sections; method I and III solutions belong to class 3, while the method II solutions belong to class 2.

The active and inactive boundary conditions are considered next. The lateral-torsional buckling was active boundary condition for all the Pareto-optimal specimens. The boundary imposed by the bending moment was inactive; the largest bending moment values did not exceed the 41.5% of the permissible

https://doi.org/10.1017/dsd.2020.44 Published online by Cambridge University Press

value. Lastly, the influence of shear was practically insignificant, ranging up to 5% of the permissible value.

Based on the presented results, it can be concluded that all three methods offer nearly identical results when used as objective functions. It must be stressed that this means that all three methods predict the changes in the cost in the same way (not to be confused with costing analysis accuracy). Thus, for optimisation purposes, it is advisable to select the simplest calculation method, as it will result in faster coding and lower computational costs.

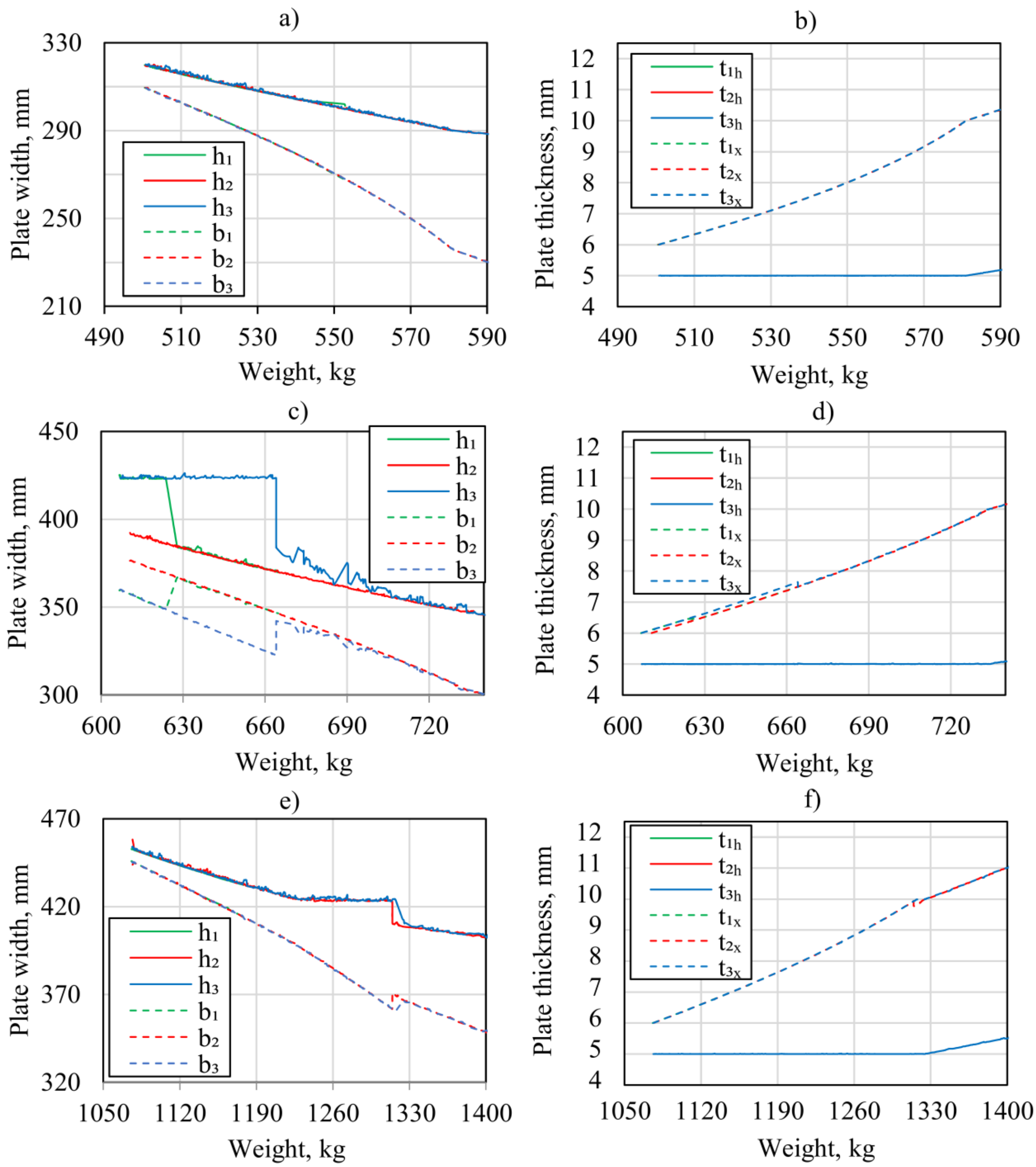

Figure 4. Optimisation results

Finally, the research question can be answered. Based on the results acquired by carrying out three identical optimisation processes (apart from cost calculation function), we conclude that:

https://doi.org/10.1017/dsd.2020.44 Published online by Cambridge University Press

- The differences caused by the cost calculation method between three considered methods are not significant. The methods evaluate relative differences between the unit cost in a similar manner, resulting in nearly identical sets of Pareto optimal solutions. However, slight variations are found in the parts of the Pareto optimal front where the cross-section class changes.
- The computational cost can be excluded from the calculations; it was rather short (63 s) when compared to modelling time, which can take hours. Furthermore, methods have different levels of complexity, which further influences the modelling time. Thus, it is recommended to select the simplest one of the methods.
- The optimisation process outcomes depend on the selection of various factors, such as material or fabrication cost factor. Those factors could be considered differently depending on the method, altering the results in the process. For this reason, caution is advised when selecting the factor values.

Limitations and outlook

The presented study aimed to find out whether there is a basis for future research on variations caused by the cost calculation methods as objective functions. Thus, a simpler mathematical model was used - the design space was limited to welded I-profiles, each made of three plates (two flange plates and a web) without the additional stiffeners. Also, when dealing with the gantry crane optimisation, it is recommended to include welded box beams into consideration. The main reason is the lateral-torsional buckling, which was an active boundary condition or all the optimal solutions. Since closed cross-section beams are significantly more resistant to buckling, this could result in a higher quality solution.

As a direction for future work, the authors aim to focus on the steel structure design optimisation. The first step includes the increase of the beam model geometrical complexity. The new model will allow the algorithm to change the web shape, aiming to reduce the self-weight. In addition to the increased web complexity, welded box beams will be included in the solution space. Resulting optimisation problem will, however, require a substantial increase in the number of design variables, significantly increasing the computational cost.

Regarding the cost calculation influence, further work is also intended. The focus of the following studies will be on cost division within the calculation. Each of the components will be assessed separately, allowing for a more thorough method comparison.

5. Conclusion

A research study of the cost calculation method's impact on the beam cross-section geometry was carried out. A steel beam with a welded I-profile section served as an example. The optimisation process was multi-objective, with the beam mass and cost as objective functions. Boundary conditions ensured that resulting solutions comply with the European standard requirements. The process was carried out three times, using different cost calculation method every time. The *non-dominated search genetic algorithm II* was used to find the solutions.

The results have pointed out to the limited influence of the cost calculation method. All considered methods displayed uniform results regarding the flange and web thickness selection. However, the limited differences were found in plate dimensions, mostly near the cross-section class changes (from 2 to 3). A higher height-to-width ratio of the class 3 cross-sections results in lower lateral-torsional buckling resistance. The class 2 profiles are calculated according to the plastic section resistance, compared to elastic in class 3 profiles.

When compared to their use in cost prediction, the absolute value is not as crucial in optimisation. Since all units within the design space are assessed using the same objective function, only relative differences matter. Thus, based on the Pareto fronts, we concluded that variations between the considered methods are not significant when used for beam optimisation. The choice between the calculation methods can be made according to the calculation complexity - this way, the preparation times and computational cost can be reduced.

Nomenclature

Variable	*Unit*	*Description*
A_v	mm2	Shear area
A_w	mm2	Area of a web
C_M	-	Material cost
F_Q	N	Load weight
f_y	MPa	Yield strength
G	N	Weight
I_y	mm4	Cross-section moment of inertia (around y-axis)
k_f	-	Fabrication cost factor
k_m	-	Material cost factor
$M_{b,RD}$	Nm	Design buckling resistance moment
$M_{c,RD}$	Nm	Design resistance for bending about one principal axis of a cross-section
M_{eD}	Nm	Design bending moment
$V_{c,RD}$	N	Design shear resistance
V_{eD}	N	Design shear force
w	mm	Beam deflection
w_{perm}	mm	Permissible beam deflection
W_y	mm3	Cross-section modulus
γ_{M0}	-	Partial factor for resistance of cross-sections whatever the class is
γ_{M1}	-	Partial factor for resistance of members to instability assessed by member checks
χ_{LT}	-	Reduction factor for lateral-torsional buckling

References

Ahmid, A., Le, V. and Dao, T.M. (2017), "An Optimization Procedure for Overhead Gantry Crane Exposed to Buckling and Yield Criteria", *IRA International Journal of Technology and Engineering*, Vol. 8, pp. 28-38.

Arora, J.S. (2017), *Introduction to optimum design*, 4. ed. Elsevier, London.

Deb, K. et al. (2002), "A fast and elitist multiobjective genetic algorithm: NSGA-II". *IEEE Transactions on Evolutionary Computation*, Vol. 6 No. 2, pp. 182-197.

EN 1993-1 (2005), *Eurocode 3: Design of steel structures*, s.l.: European Committe for Standardization.

Haapio, J. (2012), *Feature-based costing method for skeletal steel structures based on the process approach* (*PhD thesis*). s.l.: Tampere University of Technology.

Jarmai, K. and Farkas, J. (1999), "Cost calculation and optimisation of welded steel structures", *Journal of Constructional Steel Research*, Vol. 50, pp. 115-135.

Leng, J., Guest, J.K. and Schafer, B.W. (2011), "Shape optimization of cold-formed steel columns", *Thin-Walled Structures*, Vol. 49, pp. 1492-1503.

Mela, K. and Heinisuo, M. (2014), "Weight and cost optimization of welded high strength steel beams", *Engineering Structures*, Vol. 79, pp. 354-364.

Miler, D. et al. (2018), "Multi-objective spur gear pair optimization focused on volume and efficiency", *Mechanism and Machine Theory*, Vol. 125, pp. 185-195.

Ozbasaran, H. (2018), "Optimal design of I-section beam-columns with stress, non-linear deflection and stability constraints", *Engineering Structures*, Vol. 171, pp. 385-394.

Pavlovčič, L., Krajnc, A. and Beg, D. (2004), "Cost function analysis in the structural optimization of steel frames", *Structural and Multidisciplinary Optimization*, Vol. 28, pp. 286-295.

Sawulski, J. and Ławryńczuk, M. (2019), "Optimization of control strategy for a low fuel consumption vehicle engine", *Information Sciences*, Vol. 493, pp. 192-216.

https://doi.org/10.1017/dsd.2020.44 Published online by Cambridge University Press